MethodsX 9 (2022) 101611

Contents lists available at ScienceDirect

MethodsX

journal homepage: www.elsevier.com/locate/mex

Method Article

Nitrocellulose redox permanganometry: A simple method for reductive capacity assessment

Jan Homolak[a,b,*], Ivan Kodvanj[a,b], Ana Babic Perhoc[a,b], Davor Virag[a,b], Ana Knezovic[a,b], Jelena Osmanovic Barilar[a,b], Peter Riederer[c,d], Melita Salkovic-Petrisic[a,b]

[a] Department of Pharmacology, University of Zagreb School of Medicine, Zagreb, Croatia
[b] Research Centre of Excellence, Institute of Fundamental Clinical and Translational Neuroscience, Croatian Institute for Brain Research, University of Zagreb School of Medicine, Zagreb, Croatia
[c] Center of Mental Health, Department of Psychiatry, Psychosomatics and Psychotherapy, University Hospital Würzburg, Würzburg, Germany
[d] Department and Research Unit of Psychiatry, Institute of Clinical Research, University of Southern Denmark, Odense, Denmark

A B S T R A C T

We propose a rapid, simple, and robust method for measurement of the reductive capacity of liquid and solid biological samples based on potassium permanganate reduction followed by trapping of manganese dioxide precipitate on a nitrocellulose membrane. Moreover, we discuss how nitrocellulose redox permanganometry (NRP) can be used for high-throughput analysis of biological samples and present HistoNRP, its modification used for detailed analysis of reductive capacity spatial distribution in tissue with preserved anatomical relations.

- NRP is a rapid, cost-effective, and simple method for reductive capacity assessment
- NRP is compatible with a high-throughput screening of solid and liquid biological samples
- HistoNRP exploits passive diffusion slice print blotting for reductive capacity spatial analysis

A R T I C L E I N F O
Method name: Nitrocellulose Redox Permanganometry (NRP)
Keywords: Oxidative stress, Antioxidant, Reductive capacity, Nitrocellulose, Potassium permanganate, ROS
Article history: Received 9 July 2021; Accepted 29 November 2021; Available online 22 December 2021

* Corresponding author at: Department of Pharmacology, University of Zagreb School of Medicine, Zagreb, Croatia.
E-mail address: homolakjan@gmail.com (J. Homolak).

https://doi.org/10.1016/j.mex.2021.101611

Specifications table

Subject Area:	Agricultural, Biological, Chemical, and Biomedical Sciences
More specific subject area:	Redox chemistry
Method name:	Nitrocellulose Redox Permanganometry (NRP)
Name and reference of original method:	NRP is the original method based on the concept of $KMnO_4$ redox titration for determination of antioxidant capacity described by [1,2]. Novelty of NRP is the concept of utilizing nitrocellulose-trapped MnO_2 for quantification of $KMnO_4$ reduced by biological samples.
Resource availability:	Nitrocellulose membrane (GE Healthcare Life Sciences, USA); Potassium permanganate (Merck, USA).

Under physiological conditions, cellular homeostatic machinery keeps the production and elimination of biological free radicals in balance. However, once this balance is impaired, the unconstrained accumulation of free radicals triggers pathophysiological cascades involved in the etiopathogenesis of a myriad of disorders [3–5]. Consequently, numerous methods have been developed to study the production and elimination of free radicals in biological samples. The complexity of the redox homeostatic system and problematic analysis of individual subsystems lead to the need to develop a concept of a single test that might reflect the total reductive capacity and thus provide information on the overall redox status of the sample. This information is invaluable for oxidative stress research as it often provides context for understanding whether the changes of systems involved in redox homeostasis are of etiopathogenetic or compensatory nature. Hence, total reductive capacity, often called total antioxidant capacity (TAC), has been one of the most widely used methods in oxidative stress research. Consequently, many assays have been developed to determine the TAC of biological samples, but not without limitations [1]. Most of the TAC assays are based on complex chemical reactions, require sophisticated equipment and complex sample processing techniques that can potentially introduce experimental bias. Additionally, standard methods are often time-consuming, require a relatively large amount of biological samples and, most importantly, none of the existing methods can be used for the analysis of both liquid (e.g. plasma, serum, tissue homogenate) and solid (e.g. formalin-fixed paraffin-embedded or frozen tissue samples) biological samples, let alone provide the information on anatomical distribution of reduction potentials.

Here, we propose a rapid, simple, and robust method for the measurement of reductive capacity suitable for high-throughput sample processing. The proposed method can be used to understand the anatomical distribution of tissue reductive capacity, something we believe is an invaluable piece of information in oxidative stress research. In our method, the reductive capacity of the sample is measured by its capacity to reduce potassium permanganate ($KMnO_4$) to manganese dioxide (MnO_2) in a neutral environment, but in contrast to other methods based on potassium permanganate reduction, the reaction takes place on a nitrocellulose membrane. Potassium permanganate is commonly used for redox titrations ever since the discovery of permanganometry by Margueritte in 1846 [6]. It is a strong oxidant, enters few non-redox reactions, and is therefore characterized as an ideal reactant for TAC determinations [1]. However, its use in classic redox titrations is limited by an abundant brown precipitate of MnO_2 generated by $KMnO_4$ reduction in a neutral environment that complicates the determination of the reaction endpoint [1]. In the proposed method, we used this limitation to our advantage by trapping the precipitated brown MnO_2 during the redox reaction in a nitrocellulose membrane and using the solid precipitate for quantification of sample-mediated locally reduced $KMnO_4$. MnO_2 can be used for precise quantification of reductive capacity, as previously elegantly shown by Zhou et al. [1], where increased concentrations of MnO_2 in potassium permanganate agar were used to determine the antioxidant capacity of human sera.

The schematic overview of our method is depicted in Fig. 1A and a detailed step-by-step protocol is available in **Supplement 1**. To test the linearity, accuracy, and precision of the proposed method, named nitrocellulose redox permanganometry (NRP), we used sodium thiosulfate ($Na_2S_2O_3$), a well-known reducing agent standardly used for TAC method validation. Briefly, we independently prepared 10 stock solutions with nominal concentrations of 0.1 – 0.01 M (Fig. 1B) (and explained in detail in **Supplement 2**) and tested the method by using the validation criteria adopted from the official European Medicines Agency Bioanalytical Method Validation guidelines [7]. To assure the

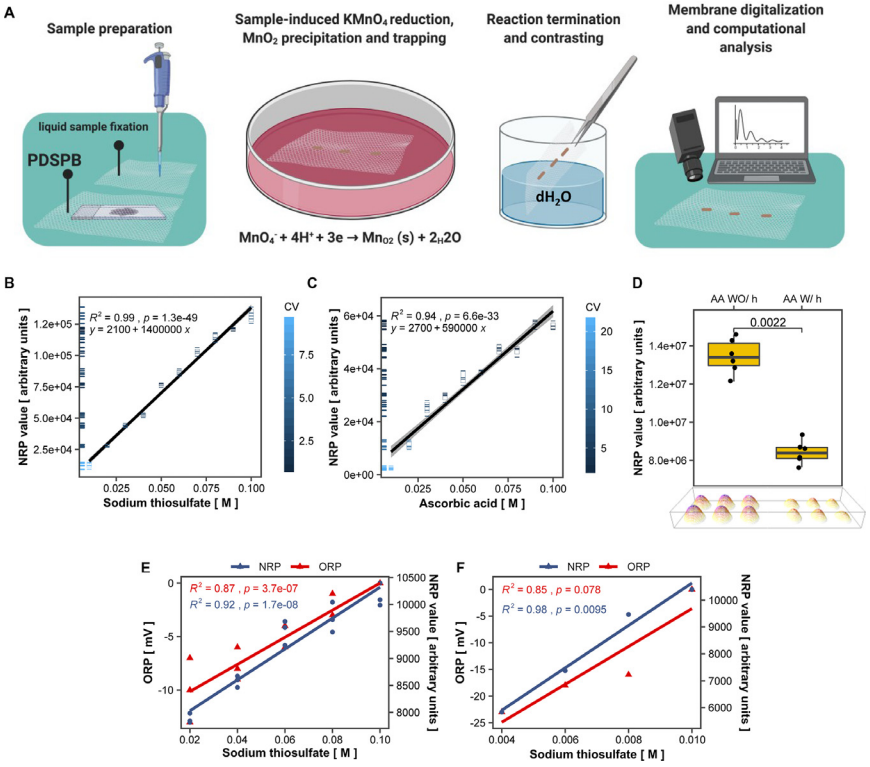

Fig. 1. Validation of nitrocellulose redox permanganometry (NRP). (**A)** Schematic step-by-step overview of NRP. First, samples of interest are fixed onto a clean sheet of nitrocellulose. Liquid samples (chemical solutions, serum, plasma, tissue homogenates) are fixed onto the membrane by pipetting 1 µl of sample and leaving the membrane to air-dry. Solid samples (formalin-fixed paraffin-embedded (FFPE) tissue samples and cryosections) are fixed onto nitrocellulose by enzymatic retrieval followed by heat-facilitated passive diffusion slice printing for FFPE or passive diffusion slice print blotting (PDSPB) for cryosections (described in detail in **Supplement 1**). After drying, the membrane is immersed in a potassium permanganate solution (63.27 mM in ddH_2O) for 30 sec. The reaction is terminated by placing the membrane in dH_2O until the contrast is maximized and the membrane is left to dry out. Once dry, the nitrocellulose sheet is digitalized and analyzed. (**B)** Validation of NRP by $Na_2S_2O_3$. Ten stock solutions of $Na_2S_2O_3$ (0.01-0.1 M) were independently prepared and fixed onto a nitrocellulose membrane. Each concentration was applied to the membrane 5-6 times and the membrane was analyzed by the protocol described in A). The integrated intensity of all dots was calculated in Fiji and statistically analyzed and visualized in R. Accuracy, precision, and linearity were calculated and are available in **Supplement 2.** All points were colored by the coefficient of variation (CV) for respective concentrations. Individual data points were additionally represented on the y axis by ticks color-coded by their CV. (**C)** Validation of NRP by ascorbic acid. In short, the whole procedure described in B) was repeated with independently prepared stock solutions of ascorbic acid (0.01-0.1 M). **D)** Validation of NRP with physically oxidized isoconcentrated samples of ascorbic acid. Briefly, we independently prepared six solutions of 0.05 M ascorbic acid and aliquoted each sample in two Eppendorf tubes. One of the two aliquots was placed at 4 °C and the other in a heating block at 70 °C. After 4 h, both aliquots were left to acclimate to room temperature and then 1 µl of each solution was placed on a clean sheet of nitrocellulose membrane. Once dry, the membrane was analyzed by the protocol described in A). The integrated intensity of all dots was calculated in Fiji and statistically analyzed and visualized in R. Fire lookup Table 3D intensity surface plot of raw images is presented at the bottom of the graph. Ascorbic acid oxidation validation was additionally tested with respect to time and temperature (all experiments are available in **Supplement 3**). AA – ascorbic acid; WO/h – without heating; W/h – with heating. (**E)** Comparison of platinum microelectrode-measured direct electrochemical oxidation-reduction potential (ORP) with NRP. Five graded nominal concentrations of $Na_2S_2O_3$ were prepared and measured with ORP and NRP. Both tests were performed in triplicates (additional replications are available in **Supplement 7**). Coefficient of determination (R^2) and p values were calculated for both methods. Statistical analysis and visualization were conducted with R. **F)** The tested nominal concentrations of $Na_2S_2O_3$ (from E) were used for exogenous redox manipulation of a single biological specimen (hippocampal homogenate). In short, 9 µl of tissue homogenate was aliquoted in separate tubes, vortexed, spun down, and treated with 1 µl of ddH_2O or one of the nominal solutions of $Na_2S_2O_3$ described in the previous experiment. All samples were vortexed, spun down, and analyzed with ORP and NRP to compare the linearity and sensitivity of both methods to slight redox manipulations in a biological system. The coefficient of determination was calculated for both methods (additional replications are available in **Supplement 7**).

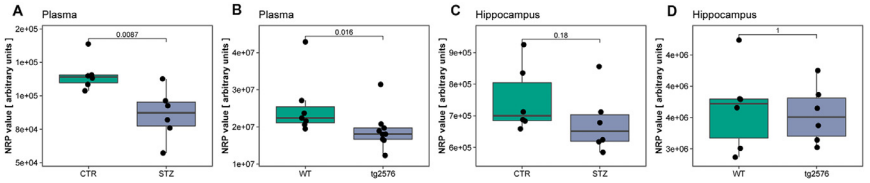

Fig. 2. Demonstration of nitrocellulose redox permanganometry (NRP). (**A)** Comparison of plasma reductive capacity of rats treated intracerebroventricularly with streptozotocin (STZ-icv) 1 month after the treatment (detailed description of the experiment is available in **Supplement 8**). Plasma samples were placed on a nitrocellulose membrane in a volume of 1 µl. Once dry, the membrane was analyzed using the protocol described in the main text, digitalized, and the integrated density of the signal was calculated for every sample in Fiji software using the gel analyzer tool. Groups were compared by Wilcoxon rank-sum test using R. (**B)** The procedure described in (A) was repeated with plasma samples of transgenic animals (Tg2576) and their wild-type controls (detailed description of the experiment is available in **Supplement 8**). **(C)** Hippocampal reductive potential was measured in tissues of the same animals from (A). In short, hippocampal homogenates were placed on a nitrocellulose membrane and the same protocol was followed as described in (A). After integrated density values were calculated, protein content correction was done utilizing ratiometric normalization (the analysis of the ratiometric protein correction approach is available in **Supplement 9**). (**D)** Hippocampal reductive potential was measured in tissues of the same animals described in (B). In short, hippocampal homogenates were placed on a nitrocellulose membrane and the same protocol was followed as described in (A). After integrated density values were calculated, protein content correction was done by means of ratiometric normalization**.**

results were not specific for $Na_2S_2O_3$ and that they truly reflected antioxidant capacity, the whole procedure was repeated with another standard reducing agent, ascorbic acid (AA) (Fig. 1C). Graded nominal concentrations of classic antioxidants are standardly used for the validation of TAC methods. However, we believe graded standards suffer from vulnerability to chemical concentration bias, so we introduced an additional test with physically oxidized isoconcentrated samples of AA (Fig. 1D). Further validation of the observed effect was done by time and temperature response analysis of AA oxidation (**Supplement 3)**. As results of both validation protocols suggested NRP to be a robust and precise method for reduction capacity assessment, additional tests were done to identify an optimal signal quantification protocol. We analyzed NRP membrane stability (**Supplement 4**) as well as potential differences in membrane digitalization techniques that could affect signal quantification (**Supplement 5**). Regarding the computational analysis of signal intensity, a method relying on the Fiji (NIH, USA) Gel Analyzer plugin was determined to be the best. The protocol is explained in **Supplement 6**. After all validation standards were fulfilled, we wanted to verify whether the same principles demonstrated with simple chemical samples can also be applied to chemically complex biological systems. To do this, we measured the direct oxidation-reduction potential (ORP) of graded nominal concentrations of $Na_2S_2O_3$ by a redox microsensor system composed of a platinum sensing element and an Ag/AgCl reference and compared these measurements to NRP results of the same $Na_2S_2O_3$ samples (Fig. 1E). We then used these samples for exogenous manipulation of one biological specimen (hippocampal homogenate) to create an experimental set with subtle reduction potential grading. We proceeded to test this experimental set by both ORP and NRP measurements (Fig. 1F).

After showing that NRP is compatible with reductive capacity measurements of biological specimens, we moved on to demonstrate the method on animal samples from our previous experiments (described in detail in **Supplement 8**). Here, we used two common models of Alzheimer's disease, a rat model of sporadic Alzheimer's disease (sAD) induced by intracerebroventricular streptozotocin (STZ-icv) treatment and the transgenic Tg2576 mouse model of familial Alzheimer's disease. It has been repeatedly shown that oxidative stress plays a pathogenic role in both models. As expected, NRP confirmed that TAC was reduced in the plasma of both models (Fig. 2A,B). We proceeded to test the TAC of hippocampal samples. Here, we needed to control for the amount of protein in each sample, as the same volume (1 µl) of all samples was pipetted to the nitrocellulose membrane for more precise and convenient analysis. As simple ratiometric correction assumes a linear relationship between NRP and protein content, this was tested before analysis with sampling-

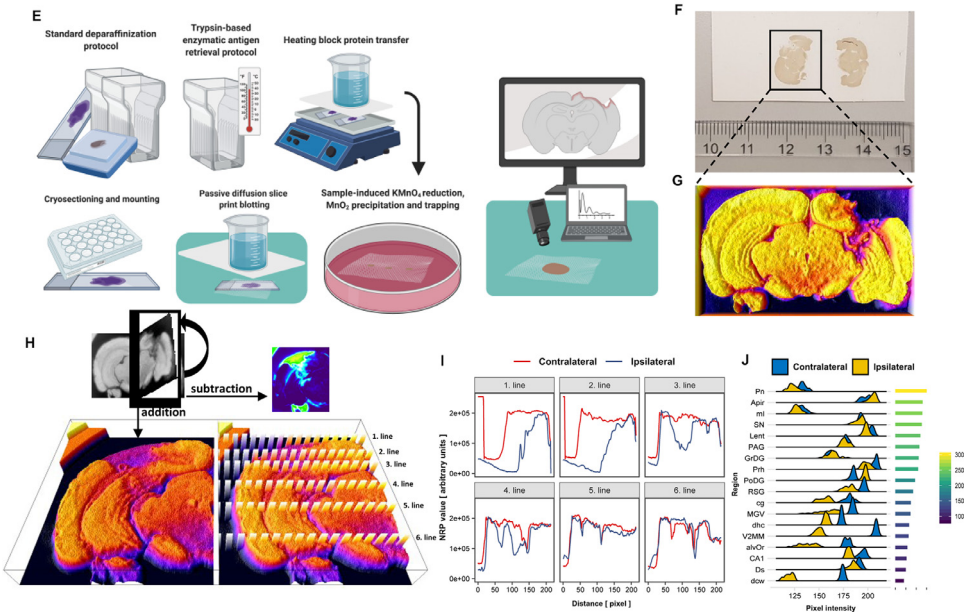

Fig. 2 Continued. (**E**) Schematic step-by-step overview of the NRP protocol adapted for analysis of histological specimens (HistoNRP). Briefly, formalin-fixed paraffin-embedded tissue (FFPE) is fixed onto a membrane by heat-facilitated passive diffusion slice printing, and cryosections are transferred onto nitrocellulose by means of passive diffusion slice print blotting. FFPE tissue is treated by standard deparaffinization protocol, followed by trypsin-based enzymatic antigen retrieval protocol, as commonly used for immunohistochemistry. After enzymatic digestion, the tissue is placed on a glass plate on a heating block. The nitrocellulose membrane is placed on tissue sections wetted with phosphate-buffered saline (PBS) and covered with three wet filter papers, and the entire setup is covered with Parafilm® and an additional glass plate. The heating block is set at 60 °C and an 800 g weight is placed on top of the upper glass plate. The transfer is stopped after 8 h (**Supplement 1, Supplement 10**), the membrane is wetted with PBS, carefully removed from the microscope slides, and dried out. Once dry, the membrane is treated with the standard NRP protocol described earlier. For cryosections, once the tissue is mounted on the microscope slide and air-dried at 37 °C, the slides are placed on a clean laboratory surface and wetted with PBS. A clean sheet of nitrocellulose membrane is placed on top of the slides and covered with three filter papers pre-wetted with PBS. The filter papers are covered with a glass plate and an 800 g weight is placed on top of the plate and left overnight. The next day, the weight and filter papers are removed, and the membrane is wetted with PBS, carefully removed from the slides, and left to air-dry. Once dry, the membrane is treated with the standard NRP protocol described earlier. (**F**) An example of a nitrocellulose membrane of brain cryosections obtained by HistoNRP (a detailed description of the experiment is available in **Supplement 8**). (**G**) A brain cryosection used for the demonstration of the anatomical distribution of reductive capacity. The HistoNRP membrane was digitalized and analyzed in Fiji software. First, the image was turned to grayscale and inverted so pixel intensity represents reductive capacity. The fire lookup table-based 3D intensity surface plot is pictured. The section was chosen for demonstration due to evident brain damage caused by microdialysis probe placement. (**H**) In order to analyze the reductive potential difference on the ipsilateral and contralateral side of the brain, the original photomicrograph was divided across the medial line. Sagittal mirroring of the damaged (ipsilateral) to control (contralateral) side was performed and intensity analysis was done by pixel addition and subtraction. The summation image is presented as a fire lookup table-based 3D intensity surface plot (bottom left). Lines of interest for the analysis of dorsoventral reductive capacity distribution were selected and visualized (bottom right). (**I**) Pixel intensity profile plots of ipsilateral and contralateral contribution values were calculated and presented for each line of interest in dorsoventral orientation. (**J**) We identified 18 brain areas of interest, calculated pixel intensity histograms for all areas on the ipsilateral and contralateral side of the brain, and measured pixel distances from ipsilateral areas to the trauma site. Ipsilateral and contralateral pixel value density plots of all areas were sorted by their distance to the trauma site (visualized in the legend on the right) to examine whether areas closest to the trauma site were also the ones with the greatest oxidative increment. **Pn** – paranigral nucleus; **Apir** – amygdalopiriform transition area; **ml** – medial lemniscus; **SN** – substantia nigra; **Lent** – lateral entorhinal cortex; **PAG** – periaqueductal gray area; **GrDG** – granular dentate gyrus; **Prh** – perirhinal cortex; **PoDG** – polymorph layer of the dentate gyrus; **RSG** – retrosplenial granular cortex; **cg** – cingulum; **MGV** – medial geniculate nucleus, ventral part; **dhc** – dorsal hippocampal commissure; **V2MM** – secondary visual cortex, mediomedial area; **alvOr** – alveus of the hippocampus and oriend layer of the hippocampus; **CA1** – field CA1 of the hippocampus; **Ds** – dorsal subiculum; **dcw** – deep cerebral white matter.

unadjusted and sampling-corrected protein estimation techniques. Protein content correction was justified for samples that dispersed from the representative sample by less than 50% of its protein concentration value (**Supplement 9**), so adjusted hippocampal NRP values were calculated and visualized. There was no difference between Tg2576 mice and their respective controls, and STZ-icv treatment demonstrated a trend towards decreased TAC (Fig. 2C,D). In summary, NRP can be used to rapidly obtain reliable information on reductive potential from small volumes of biological samples. Due to its simplicity, the method is very robust and convenient for the parallel analysis of a large number of samples. Moreover, the method is compatible with different tissue sample preparation procedures so it can be easily combined with other analytical techniques and implemented in experimental design. However, NRP can also be adapted for analysis of the anatomical distribution of reductive potential in solid tissue samples, a feature that makes our method unique and different from all other standard methods used for TAC evaluation. The HistoNRP method overview is demonstrated (Figure 2 and 2 Continued-E) and detailed step-by-step protocols are available in **Supplement 1**. In short, proteins from tissue sections are transferred and fixed onto a nitrocellulose membrane by passive diffusion slice print blotting for cryosections and enzymatic retrieval followed by heat-facilitated passive diffusion slice printing for paraffin-embedded tissues. After the fixation of proteins with preserved anatomical relations onto the nitrocellulose membrane, standard NRP protocol is used to obtain anatomical distributions of reductive capacity based on MnO_2 precipitation patterns. A representative HistoNRP nitrocellulose membrane after passive diffusion slice print blotting of cryosections is shown in Fig. 2F (an adaptation of the HistoNRP for analysis of paraffin-embedded tissue is demonstrated in **Supplement 1** and discussed in detail in **Supplement 10**). Once digitalized, the membranes can be further analyzed to obtain detailed information on the spatial distribution of reductive capacity. For a demonstration of spatial reductive analysis, we used a rat brain damaged by microdialysis probe placement (a detailed description of the experiment can be found in **Supplement 8**). Reductive capacity distribution of the damaged side of the brain was compared to the contralateral signal to explore how trauma affected different anatomical regions. Fire lookup table-based 3D intensity surface plot of reductive potential capacity obtained with HistoNRP protocol is shown in Fig. 2G. Intensities of ipsilateral and contralateral pixels obtained by sagittal mirroring were visualized by fire lookup table-based 3D intensity surface plot (Fig. 2H**, left**) and line profiles of interest were defined and visualized in (Fig. 2H**, right**). Visual representation of individual intensity profiles from (Fig. 2H) is presented in Fig. 2I. Furthermore, brain areas of interest were identified and their intensity histograms were compared to the ones obtained from the contralateral side. Density plots of analyzed areas were sorted by their distance from the trauma site and visualized in Fig. 2J. A detailed explanation of the analysis protocol is available in **Supplement 11**. So far HistoNRP seems to provide reliable results for cryosections, however an adaptation of the protocol for the analysis of paraffin-embedded tissue (**Supplement 1, Supplement 10**) is complicated by the heating step that facilitates the transfer of molecules form the tissue onto the nitrocellulose as heat can also oxidize the tranfered samples (e.g. ascorbic acid heating-induced NRP alterations [**Supplement 3**]) or even denaturate/modify the structure of proteins and alter their antioxidant function [8]. The implications of the latter are still being explored so the proposal of HistoNRP adaptation for paraffin-embedded tissue should be taken with caution until thoroughly tested.

NRP has so far been used for measurement of plasma, duodenal, ileal and hippocampal tissue samples [9,10,[12]], interstitial and intracellular fluid enriched dermal capillary blood [11], and HistoNRP has been exploited for analysis of spatiotemporal reductive patterns in rat brain upon acute oral galactose treatment [10].

In conclusion, our results demonstrate that NRP is a rapid, cost-effective, and simple method that can be used for high-throughput analysis of reductive potential. Moreover, its extension, HistoNRP provides invaluable information on tissue distribution of reductive capacity in great detail and can be used in concordance with other methods for a thorough understanding of redox homeostasis and oxidative stress.

Declaration of Competing Interest

Authors have no conflict of interest to disclose.

Authors contributions

JH conceptualized the method, designed experimental protocols and validation tests, and conducted all NRP experiments. JH, IK, and DV conducted data analysis and visualization. JH, IK, ABP, and DV wrote the manuscript. JH, ABP, AK, and JOB conducted animal experiments from which tissue samples were taken for proof-of-concept analyses. MSP is head of the Laboratory for Molecular Neuropharmacology where all experiments were conducted, principal investigator of the Croatian Science Foundation-funded project (IP-2018-01-8938) and research group leader in the Scientific Centre of Excellence for Basic, Clinical and Translational neuroscience (GA KK01.1.1.01.0007) and supervisor and mentor of the authors. PR provided valuable comments on the manuscript and the method as a renowned expert in the field of neurochemistry and a close collaborator of the group. All authors approved the manuscript and provided comments during the writing process.

Data availability statement

All data used in the preparation of the manuscript (a total of 28 datasets) can be found on the author's GitHub repository (https://github.com/janhomolak/NRP) and in the Mendeley Data repository (10.17632/fgfpzhrxjm.1).

Ethics committee approval

All experiments were conducted in concordance with the highest standard of animal welfare. Only certified personnel handled animals. Animal procedures were carried out at the University of Zagreb Medical School (Zagreb, Croatia) and were in compliance with current institutional, national and international (The Animal Protection Act, NN 102/17, 32/19, NN 125/13, 14/14, 92/14, 32/19), and international (Directive 2010/63/EU) guidelines governing the use of experimental animals. The experiments were approved by the national regulatory body responsible for issuing ethical approvals, the Croatian Ministry of Agriculture, and the Ethical Committee of the University of Zagreb School of Medicine.

Funding source

This work was funded by the Croatian Science Foundation (IP-2018-01-8938 and IP-09-2014-4639). The research was co-financed by the Scientific Centre of Excellence for Basic, Clinical, and Translational Neuroscience (project Experimental and clinical research of hypoxic-ischemic damage in the perinatal and adult brain; GA KK01.1.1.01.0007 funded by the European Union through the European Regional Development Fund).

Supplementary materials

Supplementary material associated with this article can be found, in the online version, at doi:10.1016/j.mex.2021.101611.

References

[1] Y. Zhou, M. Zhang, H. Liu, Total antioxidant capacity of serum determined using the potassium permanganate agar method based on serum diffusion in agar, Bioinorg. Chem. Appl. 2015 (2015) 406071, doi:10.1155/2015/406071.
[2] M. Zhang, N. Liu, H. Liu, Determination of the total mass of antioxidant substances and antioxidant capacity per unit mass in serum using redox titration, Bioinorg. Chem. Appl. 2014 (2014), doi:10.1155/2014/928595.
[3] N.D. Vaziri, B. Rodríguez-Iturbe, Mechanisms of disease: oxidative stress and inflammation in the pathogenesis of hypertension, Nat. Clin. Pract. Nephrol. 2 (2006) 582–593, doi:10.1038/ncpneph0283.
[4] T. Finkel, N.J. Holbrook, Oxidants, oxidative stress and the biology of ageing, Nature 408 (2000) 239–247, doi:10.1038/35041687.
[5] K.J. Barnham, C.L. Masters, A.I. Bush, Neurodegenerative diseases and oxidative stress, Nat. Rev. Drug Discov. 3 (2004) 205–214, doi:10.1038/nrd1330.
[6] F. Szabadvary, History of Analytical Chemistry, Pergamon press, 1966.

[7] European Medicines AgencyBioanalytical Method Validation, European Medicines Agency, 2018 https://www.ema.europa.eu/en/bioanalytical-method-validation (accessed March 8, 2020).
[8] R. Medina-Navarro, G. Durán-Reyes, M. Díaz-Flores, C. Vilar-Rojas, Protein antioxidant response to the stress and the relationship between molecular structure and antioxidant function, PLoS One 5 (2010) e8971, doi:10.1371/journal.pone.0008971.
[9] J. Homolak, A. Babic Perhoc, A. Knezovic, J. Osmanovic Barilar, M. Salkovic-Petrisic, Failure of the brain glucagon-like peptide-1-mediated control of intestinal redox homeostasis in a rat model of sporadic Alzheimer's disease, Antioxidants 10 (2021) 1118, doi:10.3390/antiox10071118.
[10] J. Homolak, A.B. Perhoc, A. Knezovic, I. Kodvanj, D. Virag, J.O. Barilar, P. Riederer, M. Salkovic-Petrisic, Is galactose a hormetic sugar? An exploratory study of the rat hippocampal redox regulatory network, Mol. Nutr. Food Res. (2021) e2100400, doi:10.1002/mnfr.202100400.
[11] J. Homolak, The effect of a color tattoo on the local skin redox regulatory network: an N-of-1 study, Free Radic. Res. (2021) 1–9, doi:10.1080/10715762.2021.1912340.
[12] Jan Homolak, Ana Babic Perhoc, Ana Knezovic, Jelena Osmanovic Barilar, Davor Virag, Mihovil Joja, Melita Salkovic-Petrisic, The Effect of Acute Oral Galactose Administration on the Redox System of the Rat Small Intestine, Antioxidants (2021) In press, doi:10.3390/antiox11010037.